Diphoton hadroproduction at the NLO* level in the Parton Reggeization Approach.

M. A. Nefedov[1], V. A. Saleev[1,2]

QFTHEP-2015
Samara, 29 June 2015

[1] Samara State University, Samara, Russia
[2] Samara State Aerospace University

Outline.

Introduction

This talk is based on the results, presented in [M. A. Nefedov, V. A. Saleev, Diphoton production at Tevatron and the LHC in the NLO* approximation of the Parton Reggeization Approach; arXiv:hep-ph/1505.01718].

Diphoton production is interesting as from the point of view of the New Physics searches (e. g. irred. background to $H \to \gamma\gamma$) and also as an excellent test for the techniques in pQCD:

- Fixed-order canculations in the Collinear Parton Model (CPM)
- Soft gluon/logarithmic resummation techniques
- k_T-factorization, TMD factorization

Inclusive diphotons in pp or $p\bar{p}$ collisions.

Let's consider the reaction:

$$p(P_1) + p(P_2) \to \gamma(q_3) + \gamma(q_4) + X,$$

where the photons are **hard** ($q_{T3,4} \gtrsim 10$ GeV), **isolated** in the $(\Delta y, \Delta\phi)$ plane, both from each other, and from hadronic activity, and **prompt**, i. e. have to come from the primary collision vertex.
There are many **differential** observables to meashure:

$$\frac{d\sigma}{dM}, \frac{d\sigma}{dp_T}, \frac{d\sigma}{dY}, \frac{d\sigma}{d\Delta\phi}, \frac{d\sigma}{d\cos\theta^*}, \frac{d\sigma}{dz}, \dots ,$$

where $M^2 = (q_3 + q_4)^2$, $p_T^2 = (\mathbf{q}_{T3} + \mathbf{q}_{T4})^2$, $z = q_{T3}/q_{T4}$, θ^*- Collins angle, and the process itself is **multiscale**:

$$p_T,\ M,\ E_{Tmin}^{(L)},\ E_{Tmin}^{(SL)},\ E_T^{(ISO)}$$

Approach of the Collinear Parton Model in the fixed order.

Factorization formula of the CPM:

$$d\sigma = \sum_{p_1,p_2} \int_0^1 dx_1 \int_0^1 dx_2 f_{p_1}(x_1,\mu_F^2) f_{p_2}(x_2,\mu_F^2) d\hat{\sigma}_{p_1 p_2}(q_1,q_2,\mu_F,\mu_R),$$

where $q_1 = x_1 P_1$, $q_2 = x_2 P_2$, $P_{1,2}^2 = 0$, $f_p(x,\mu_F)$ – (integrated) PDF of the parton p in proton, $d\hat{\sigma}$ – hard-scattering cross-section. For the sufficiently inclusive **single-scale** observables (e. g. $d\sigma/dydQ^2$ in Drell-Yan), it is proven (see e. g.[Collins, 2011]), that the factorization-breaking terms are power-supressed (e. g. $\sim 1/Q^2$), and large-$\alpha_s \log(Q^2)$ perturbative corrections are resummed through the μ_F-dependence of the PDFs, using the **DGLAP** evolution equation.
The LO ($O(\alpha_s^0)$) subprocess is:

$$q + \bar{q} \to \gamma + \gamma,$$

The NLO ($O(\alpha_s^1)$) subprocesses:

$q + g \to \gamma + \gamma + q$; $q + \bar{q} \to \gamma + \gamma + g$; **1-loop virtual corrections**

NNLO ($O(\alpha_s^2)$):

$g + g \to \gamma + \gamma$; $2 \to 4$ **real**; $2 \to 3$ **real-virtual**; **2-loop virtual** corections.

Direct and fragmentation contributions.

The **experimental definition** of the σ requires no hadrons (QCD radiation) with $E_T > E_T^{(ISO)}$ in the isolation cone of the photon $\delta = \sqrt{\Delta\phi^2 + \Delta y^2} \leq R$. This definition is not **collinear-safe** due to collinear singularity of the $q \to q\gamma$ splitting. Ways out:

- Introduce the quark$\to \gamma$ FF: $f_{\gamma/q}(z, \mu^2)$, which will absorb the collinear singularity. $\Rightarrow \sigma_{obs} =$ **direct component** (with collinear singularity subtracted in the $\overline{MS}$ scheme)+ **fragmentation component**. Problems: FFs should be fitted to data and introduction of the FFs complicates the analytcs **a lot**.
- There is a way to define collinear-safe direct cros-section – **Frixione isolation condition** [Frixione, 1998].

The trick is to modify the isolation condition:

$$E_T \leq E_T^{(ISO)} \chi(\delta),\ \chi(\delta) = \left(\frac{1 - \cos\delta}{1 - \cos R} \right)^n,\ n \geq 1/2.$$

Recent studies [Cieri, de Florian, 2013] show, that the direct contribution with Frixione isolation condition ($n = 1$) is a very good (within $1 - 3\%$) estimate of the full direct+fragmentation cross-section with standard isolation at NLO. Since higher-order effects are very important ($O(100\%)$ in some kinematical regions), it is reasonable to proceed with Frixione isolation.

NLO and NNLO results, ATLAS data.

Plots are extracted from [arXiv:hep-ex/1211.1913v2]:

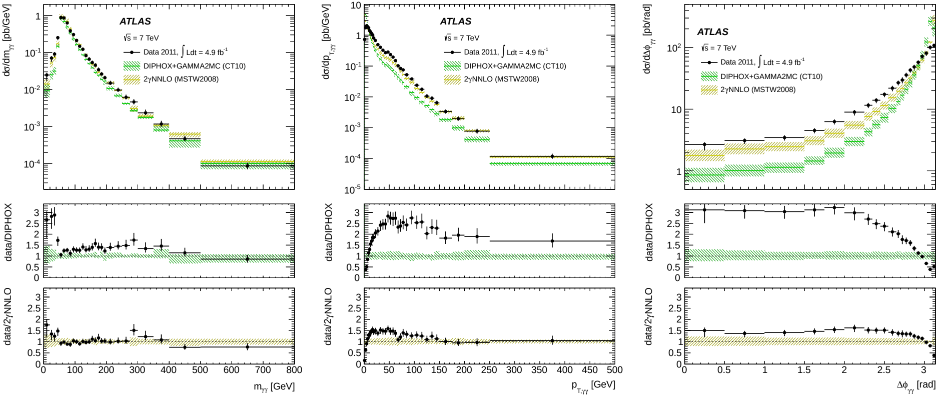

$$LO + NLO + NNLO \simeq \text{experinent} \Rightarrow N^3LO \ll NNLO \text{ ???}$$

k_T-factorization and PRA.

In the CPM, the transverse momentum $\mathbf{q}_T$ of initial-state parton is **neglected** in the hard part and **integrated over** in the PDFs. This approximation leads to large higher-order corrections to the p_T-spectra in CPM. The k_T**-factorization** scheme [Gribov *et. al.* 1983; Collins *et. al.* 1991; Catani *et. al.* 1991] is introduced to improve the description in the kinematical region where:

$$q^{\pm} = x\sqrt{S} \sim |\mathbf{q}_T| \ll q^{\mp}$$

Here, most of the initial state radiation is **highly separated in rapidity** from the central region, and can be factorized, but **the transverse-momentum of the initial-state parton can not be neglected in the hard-scattering part, and should be taken ito account in the gauge-inveriant way**.
In present time, three methods proposed to solve the last problem:

- The old k_T-factorization prescription for gluons ($\varepsilon^{\mu}(q) = \frac{q_T^{\mu}}{|\mathbf{q}_T|}$).
- The parton Reggeization approach (PRA).
- Methods based on the extraction of the multi-Regge asymptotics of the amplitudes in the spinor-helicity representation [van Hameren *et. al.*, 2013].

In fact, the last two are closely related to each-other.

Reggeization of amplitudes in QCD.

PRA is based on the Reggeization of amplitudes in gauge theories (QED, QCD, Gravity). The *high energy asymptotics* of the $2 \to 2 + n$ amplitude is dominated by the diagram with t-channel exchange of the effective (Reggeized) particle and Multi-Regge (MRK) or Quasi-Multi-Regge Kinematics (QMRK) of final state.

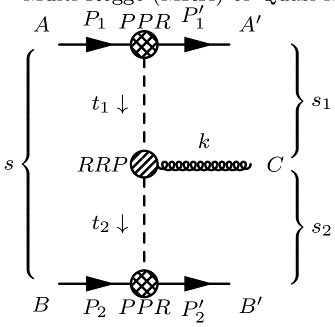

In the limit $s \to \infty$, $s_{1,2} \to \infty$, $-t_1 \ll s_1$, $-t_2 \ll s_2$ (Regge limit), $2 \to 3$ amplitude has the form:

$$\mathcal{A}_{AB}^{A'B'C} = 2s\gamma_{A'A}^{R_1} \left(\frac{s_1}{s_0}\right)^{\omega(t_1)} \frac{1}{t_1} \times$$

$$\times \Gamma_{R_1 R_2}^{C}(q_1, q_2) \times \frac{1}{t_2} \left(\frac{s_2}{s_0}\right)^{\omega(t_2)} \gamma_{B'B}^{R_2}$$

$\Gamma_{R_1 R_2}^{C}(q_1, q_2)$ - RRP effective production vertex,

$\gamma_{A'A}^{R}$ - PPR effective scattering vertex,

$\omega(t)$ - Regge trajectory.

Two approaches to obtain this asymptotics:

- BFKL-approach (Unitarity, renormalizability and gauge invariance), see e. g. [Ioffe, Fadin, Lipatov, 2010].
- Effective action approach [Lipatov, 1995].

The field content of the effective theory.

Light-cone vectors:

$$n^+ = \frac{2P_2}{\sqrt{S}},\ n^- = \frac{2P_1}{\sqrt{S}},\ n^+ n^- = 2$$

$$x^\pm = n^\pm x = x^0 \pm x^3,\ \partial_\pm = 2\frac{\partial}{\partial x^\mp}$$

Lagrangian of the effective theory $L = L_{kin} + \sum\limits_y \left(L_{QCD} + L_{ind}\right)$, $v_\mu = v_\mu^a t^a$, $\left[t^a, t^b\right] = f^{abc} t^c$. Each subinterval in rapidity $(1 \ll \eta \ll Y)$ has it's own set of QCD fields:

$$L_{QCD} = -\frac{1}{2} tr\left[G_{\mu\nu}^2\right],\ G_{\mu\nu} = \partial_\mu v_\nu - \partial_\nu v_\mu + g\left[v_\mu, v_\nu\right].$$

Different rapidity intervals communicate via Reggeized gluons $(A_\pm = A_\pm^a t^a)$ with the kinetic term:

$$L_{kin} = -\partial_\mu A_+^a \partial^\mu A_-^a,$$

and the kinematical constraint:

$$\partial_- A_+ = \partial_+ A_- = 0 \Rightarrow$$

$$A_+ \text{ has } k_- = 0 \text{ and } A_- \text{ has } k_+ = 0.$$

The effective action for high energy processes in QCD.

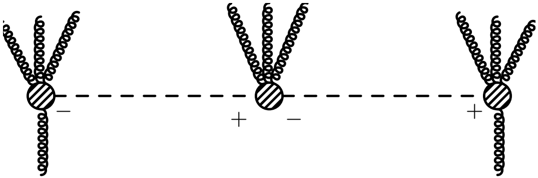

Particles and Reggeons interact via *induced interactions*:

$$L_{ind} = - tr\left\{ \frac{1}{g}\partial_+ \left[P\exp\left(-\frac{g}{2}\int\limits_{-\infty}^{x^-} dx'^- v_+(x') \right) \right] \cdot \partial_\sigma \partial^\sigma A_-(x) + \right.$$
$$\left. + \frac{1}{g}\partial_- \left[P\exp\left(-\frac{g}{2}\int\limits_{-\infty}^{x^+} dx'^+ v_-(x') \right) \right] \cdot \partial_\sigma \partial^\sigma A_+(x) \right\}$$

Wilson lines generate the infinite chain of the induced vertices:

$$L_{ind} = tr\left\{ \left[v_+ - g v_+ \partial_+^{-1} v_+ + g^2 v_+ \partial_+^{-1} v_+ \partial_+^{-1} v_+ - \ldots \right] \partial_\sigma \partial^\sigma A_- + \right.$$
$$\left. + \left[v_- - g v_- \partial_-^{-1} v_- + g^2 v_- \partial_-^{-1} v_- \partial_-^{-1} v_- - \ldots \right] \partial_\sigma \partial^\sigma A_+ \right\}$$

Feynman rules. Quarks, gluons and photons.

Feynman Rules for Reggeized gluons [Antonov, Cherednikov, Kuraev, Lipatov, 2005]
Feynman Rules for Reggeized quarks [Lipatov, Vyazovsky, 2001]

Initial state factors:

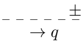

$$= \frac{q^\pm}{2\sqrt{-q^2}},$$

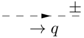

$$= u(q^\parallel).$$

Propagators ($\hat{P}_\pm = \frac{1}{4}\hat{n}^\mp\hat{n}^\pm$):

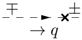

$$= \hat{P}_\pm \frac{i\hat{q}}{q^2},$$

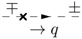

$$= \frac{i\hat{q}}{q^2}\hat{P}_\pm.$$

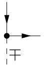

$$= -ig_s T^a \hat{n}^\pm,$$

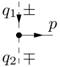

$$= -ig_s T^a \left(\hat{n}^\pm + 2\frac{\hat{q}_1}{q_2^\mp}\right),$$

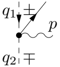

$$= -2ieg_s T^a \frac{\hat{q}_1 n_\mu^\mp}{p^\mp q_2^\mp},$$

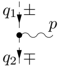

$$= -ie\left(\gamma_\mu + \hat{q}_1\frac{n_\mu^\mp}{p^\mp} + \hat{q}_2\frac{n_\mu^\pm}{p^\pm}\right),$$

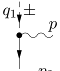

$$= -ie\left(\gamma_\mu + \hat{q}_1\frac{n_\mu^\mp}{p^\mp}\right),$$

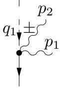

$$= -ie^2\hat{q}_1\frac{n_{\mu_1}^\mp n_{\mu_2}^\mp}{p_1^\mp p_2^\mp}.$$

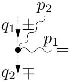

$$= ie^2\left(\hat{q}_2\frac{n_{\mu_1}^\pm n_{\mu_2}^\pm}{p_1^\pm p_2^\pm} - \hat{q}_1\frac{n_{\mu_1}^\mp n_{\mu_2}^\mp}{p_1^\mp p_2^\mp}\right),$$

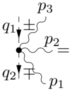

$$= -ie^3\left(\hat{q}_2\frac{n_{\mu_1}^\pm n_{\mu_2}^\pm n_{\mu_3}^\pm}{p_1^\pm p_2^\pm p_3^\pm} + \hat{q}_1\frac{n_{\mu_1}^\mp n_{\mu_2}^\mp n_{\mu_3}^\mp}{p_1^\mp p_2^\mp p_3^\mp}\right),$$

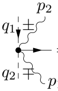

$$= -2ie^2 g_s T^a \frac{\hat{q}_1 n_{\mu_1}^\mp n_{\mu_2}^\mp}{p_1^\mp p_2^\mp q_2^\mp}.$$

Factorization of the cross-section.

Factorization:

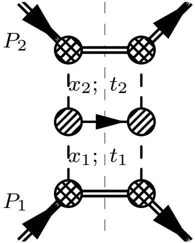

Collinear limit holds for the amplitude:

$$\int \frac{d\phi_1 d\phi_2}{(2\pi)^2} \lim_{t_{1,2}\to 0} \overline{|\mathcal{M}|^2}_{PRA} = \overline{|\mathcal{M}|^2}_{CPM}$$

k_T-factorization formula:

$$d\sigma = \int \frac{d^2\mathbf{q}_{T1}}{\pi} \int \frac{dx_1}{x_1} \Phi(x_1, t_1, \mu_F) \times$$
$$\times \int \frac{d^2\mathbf{q}_{T2}}{\pi} \int \frac{dx_2}{x_2} \Phi(x_2, t_2, \mu_F) d\hat{\sigma}_{PRA}$$

Where Φ - Unintegrated PDFs. The factorization is known to hold in the LLA ($\alpha_s \log(1/x)$) [**BFKL**, 1978], and NLLA ($\alpha_s^2 \log(1/x)$) [Fadin, Lipatov, 1998; Camici, Ciafaloni, 1998; Bartels, *et. al.*, 2006].

Normalization of the unPDF:

$$\int^{\mu^2} dt \Phi(x, t, \mu^2) = x f(x, \mu^2),$$

where $f(x, \mu^2)$ - collinear PDF.

Subprocesses in the PRA.

- LO ($O(\alpha_s^0)$):
$$Q(q_1) + \bar{Q}(q_2) \to \gamma(q_3) + \gamma(q_4), \tag{1}$$
where $Q(\bar{Q})$-Reggeized quark (antiquark), $q_{1,2} = x_{1,2}P_{1,2} + q_{T1,2}$, $q_{1,2}^2 = -t_{1,2}$.
- NLO ($O(\alpha_s^1)$):
$$Q(q_1) + R(q_2) \to \gamma(q_3) + \gamma(q_4) + q(q_5), \tag{2}$$
$$Q(q_1) + \bar{Q}(q_2) \to \gamma(q_3) + \gamma(q_4) + g(q_5), \tag{3}$$
where R- Reggeized gluon. Also the 1-loop real-virtual corrections to 1 should be included.
- NNLO ($O(\alpha_s^2)$):
$$R(q_1) + R(q_2) \to \gamma(q_3) + \gamma(q_4), \tag{4}$$
$$\ldots$$

$Q\bar{Q} \to \gamma\gamma$ subprocess.

$Q_- \; Q_+ \;\to\; \gamma \;\; \gamma$

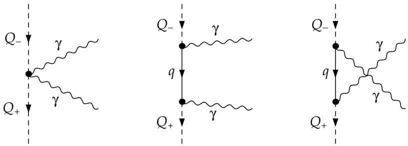

The answer is known for a long time [Saleev, 2009]:

$$\overline{|M(Q\bar{Q} \to \gamma\gamma)|^2} \quad = \quad \frac{32}{3}\pi^2 e_q^4 \alpha^2 \frac{x_1 x_2}{a_3 a_4 b_3 b_4 S \hat{t}\hat{u}} \Big(w_0 + w_1 S + w_2 S^2 + w_3 S^3 \Big),$$

where $a_3 = q_3^+/\sqrt{S}$, $a_4 = q_4^+/\sqrt{S}$, $b_3 = q_3^-/\sqrt{S}$, $b_4 = q_4^-/\sqrt{S}$, $\hat{s} = (q_1 + q_2)^2$, $\hat{t} = (q_1 - q_3)^2$, $\hat{u} = (q_1 - q_4)^2$, $x_1 = a_3 + a_4$, $x_2 = b_3 + b_4$,

$$w_0 = t_1 t_2 (t_1 + t_2) - \hat{t}\hat{u}(\hat{t} + \hat{u}),$$

$$\begin{aligned} -w_1 \quad &= \quad t_1 t_2 (a_3 - a_4)(b_3 - b_4) + t_2 x_1 (b_4 \hat{t} + b_3 \hat{u}) + \\ &+ \quad t_1 x_2 (a_3 \hat{t} + a_4 \hat{u}) + \hat{t}\hat{u}(a_3 b_3 + 2 a_4 b_3 + 2 a_3 b_4 + a_4 b_4), \end{aligned}$$

$$-w_2 = b_3 b_4 x_1^2 t_2 + a_3 a_4 x_2^2 t_1 + a_3 b_4 \hat{t}(x_1 b_3 + a_4 b_4) + a_4 b_3 \hat{u}(a_3 b_3 + a_4 x_2),$$

$$-w_3 = a_3 a_4 b_3 b_4 \left(a_3 b_4 \left(\frac{\hat{t}}{\hat{u}} \right) + a_4 b_3 \left(\frac{\hat{u}}{\hat{t}} \right) \right).$$

$QR \to \gamma\gamma q$

$$Q_- \quad R_+ \quad \to \quad \gamma \quad \gamma \quad q$$

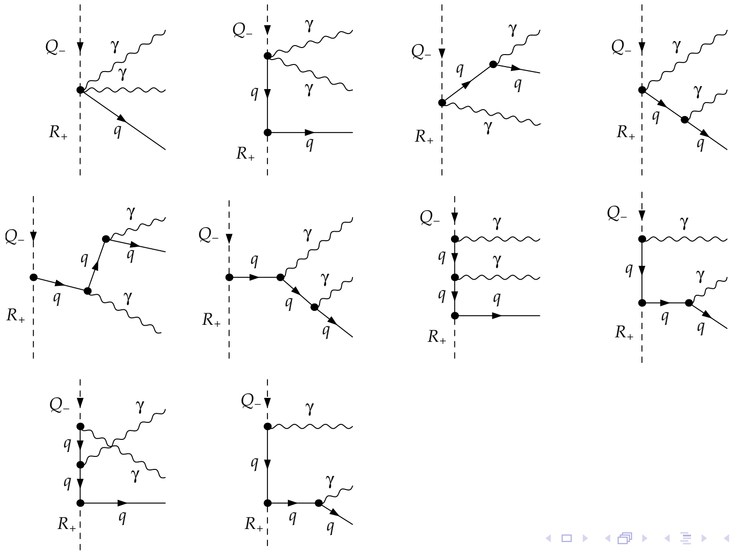

$Q\bar{Q} \to \gamma\gamma g$

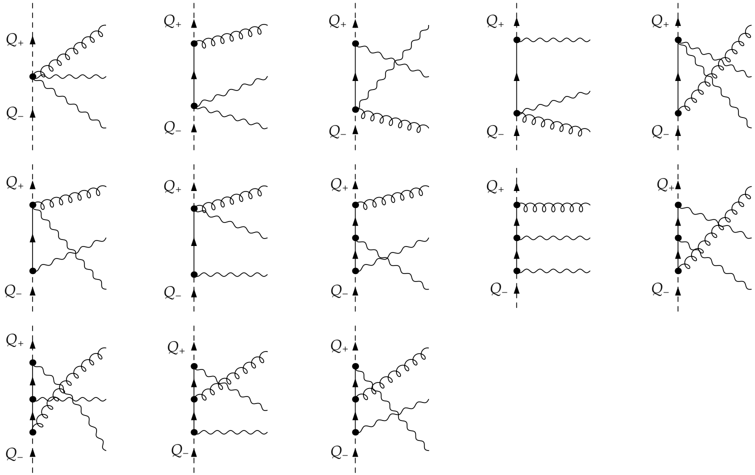

LO/NLO double counting.

The integral over the whole phase-space of the additional parton in the $2 \to 3$ subprocesses is **finite** (unlike the CPM case), due to the Sudakov suppression of the region of small-q_T in the KMR unPDF (which will be discussed below). However, there is a double-counting between LO and NLO real corections, when the additional parton goes deeply to the forward or backward rapidity regions. This double-counting should be subtracted. The appropriate subtraction technique was introduced in [Bartels, *et. al.*, 2006; Hentshinski, Vera, 2012].

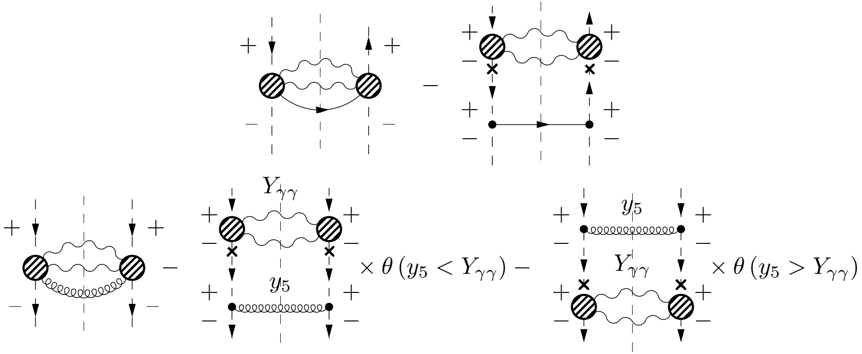

QMRK vs. MRK. Numerical results.

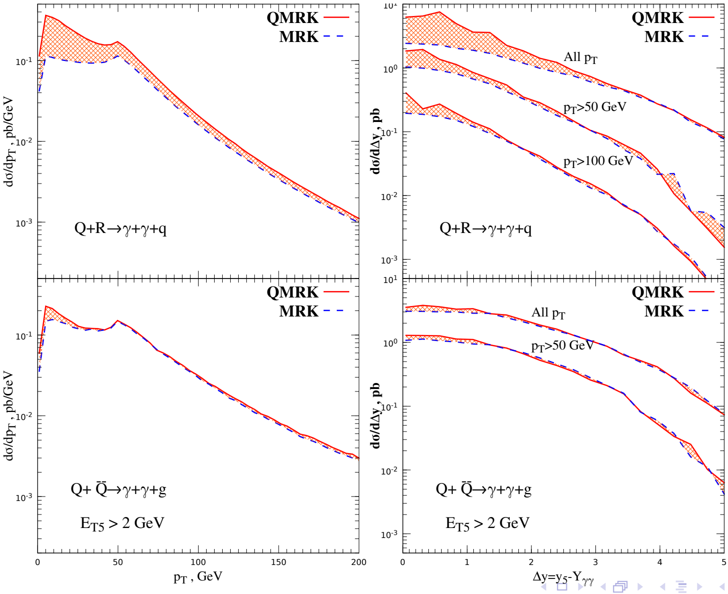

Why region of high-p_T is MRK-dominated at NLO?

Because:

- "$\hat{s}$-channel" and "$\hat{u}$-channel" contributions are power-suppressed like $\sim 1/p_T^2$.

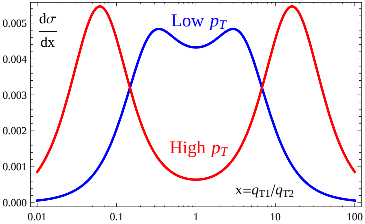

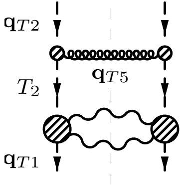

- At high-p_T, the asymmetric initial states with $p_T \sim |\mathbf{q}_{T1}| \gg |\mathbf{q}_{T2}|$ dominate.
- The T_2 invariant:

$$T_2 = -(\mathbf{q}_{T2} - \mathbf{q}_{T5})^2 - |\mathbf{q}_{T5}|\sqrt{M^2 + p_T^2} e^{-\Delta y},$$

  is minimal when $\mathbf{q}_{T2} \simeq \mathbf{q}_{T5}$ and $\Delta y \to \infty$ (Multi-Regge region).
- Therefore the MRK-configurations with:

$$p_T \sim |\mathbf{q}_{T1}| \gg |\mathbf{q}_{T2}| \simeq |\mathbf{q}_{T5}|,$$

  dominate at high-p_T and low-M, i. e. in the $M < p_T$ **region**.

The Kimber-Martin-Ryskin unPDF.

In the present numerical computations we use the modified KMR unPDF from [Martin , Ryskin, Watt 2010].
KMR prescription to obtain unintegrated PDF from collinear one is based on the mechanism of last step parton k_T-dependent radiation and the assumption of strong angular ordering:

$$\Phi_q(x,k_T^2,\mu^2)=\frac{1}{k_T^2}\int\limits_x^{1-\Delta} dz T_q(q^2,\mu^2)\frac{\alpha_s(q^2)}{(2\pi)}\left[P_{qg}(z)f_g\left(\frac{x}{z},q^2\right)+P_{qq}(z)f_q\left(\frac{x}{z},q^2\right)\right],$$

where $P_{qg}(z)$, $P_{qq}(z)$- LO DGLAP splitting functions, $T_q(k^2,\mu^2)$- Sudakov formfactor:

$$T_q(k^2,\mu^2)=exp\left\{-\int\limits_{k^2}^{\mu^2}\frac{dq_T^2}{q_T^2}\frac{\alpha_s(q_T^2)}{2\pi}\sum_{a'}\int\limits_0^{1-\Delta}P_{qa'}(z')dz'\right\}$$

where $\Delta=\frac{k_T}{\mu+k_T}$ ensures the **rapidity ordering of the last emission and particles produced in the hard subprocess**, and $q^2=k_T^2/(1-z)$.

The $RR \to \gamma\gamma$ contribution.

The $RR \to \gamma\gamma$ contribution is formally NNLO, but it is sizable, due to the enchancement of the gluon distribution at small-x. We have computed this contribution, keepinging the **exact** dependence on the virtuality of the initial-state partons, which was done for a first time. The main conclusion is the same as in the case of $\gamma R \to \gamma g$ subprocess in $\gamma p \to \gamma X$ [Kniehl, Nefedov, Saleev, 2014], the transverse momentum of the initial-state partons leads to the $30-40\%$ **suppression** of the loop-induced contributions w. r. t. corresponding CPM results.

$$R_- \; R_+ \to \gamma \; \gamma$$

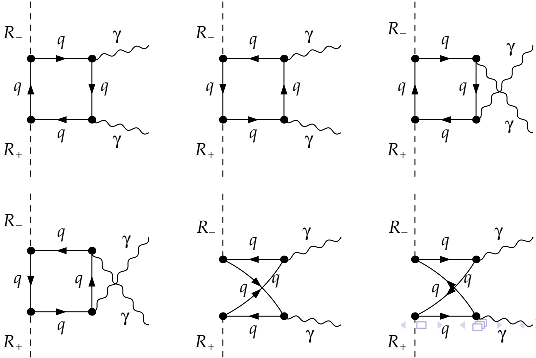

Tevatron ($p\bar{p}$, $\sqrt{S} = 1960$ GeV), p_T-spectra.

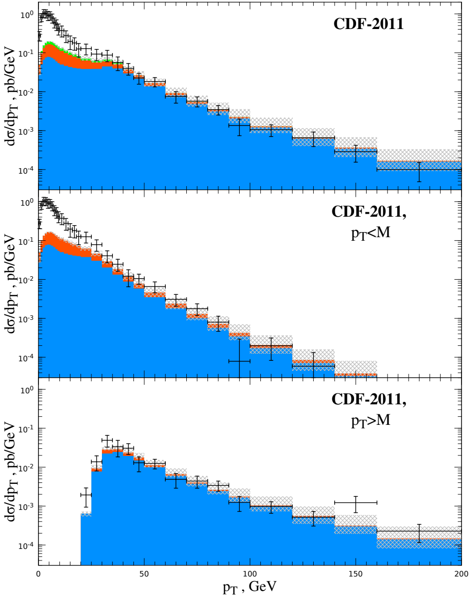

Layers of the histogram from top to bottom:

- $RR \to \gamma\gamma$
- $QR \to (\gamma\gamma)q$, QMRK-MRK
- $Q\bar{Q} \to \gamma\gamma$

Gray band – scale uncertainty:

$$\mu_R = \mu_F = \xi \max(q_{T3}, q_{T4}),$$

where $\xi = 1,\ 2^{\pm 1}$.
Contribution from the $Q\bar{Q} \to (\gamma\gamma)g$ subprocess is not shown, due to it's substantial sensitivity to E_{T5}^{min}. For $E_{T5}^{min} = 2$ GeV it is of the same order as $RR \to \gamma\gamma$, and localized at small p_T.

LHC, (pp, $\sqrt{S} = 7000$ GeV), p_T-spectra.

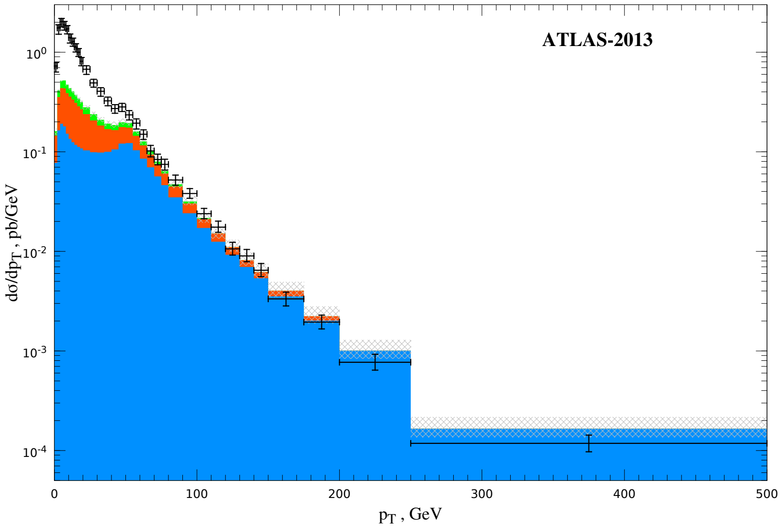

Tevatron ($p\bar{p}$, $\sqrt{S} = 1960$ GeV), $\Delta\phi$-spectra.

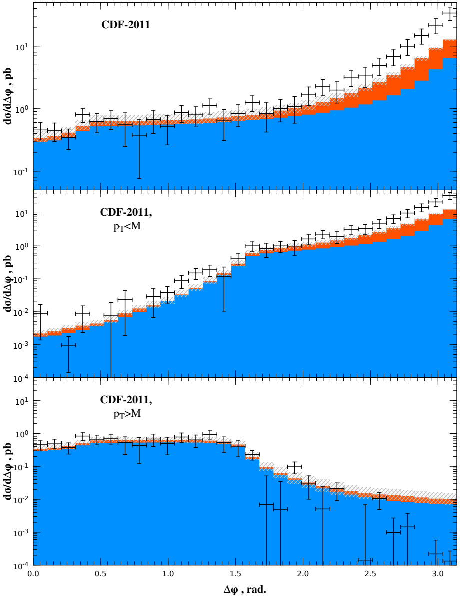

Layers of the histogram from top to bottom:

- $QR \to \gamma\gamma q$, QMRK-MRK
- $Q\bar{Q} \to \gamma\gamma$

The deficit of the theoretical cross-section is observed in the region of low p_T and $\Delta\phi \simeq \pi$, where the additional radiation is kinematically constrained to be very **soft**, this region is more suitable for the fixed-order calculations or SCET, than PRA.

LHC, (pp, $\sqrt{S} = 7000$ GeV), $\Delta\phi$-spectra.

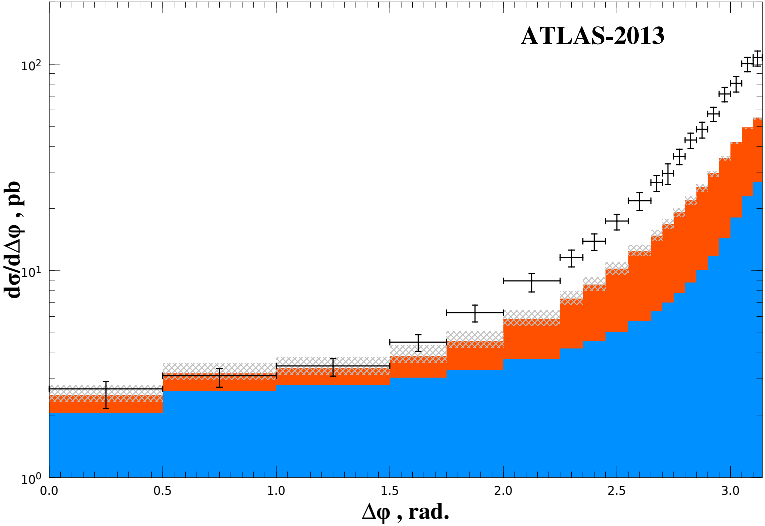

Tevatron ($p\bar{p}$, $\sqrt{S} = 1960$ GeV), M-spectra.

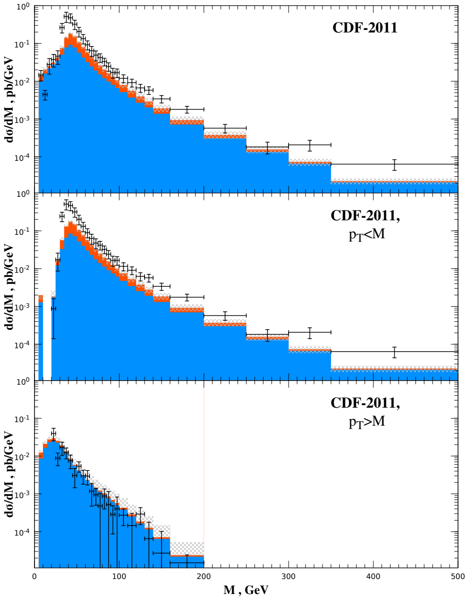

Layers of the histogram from top to bottom:

- $QR \to \gamma\gamma q$, QMRK-MRK
- $Q\bar{Q} \to \gamma\gamma$

LHC, (pp, $\sqrt{S} = 7000$ GeV), M-spectra.

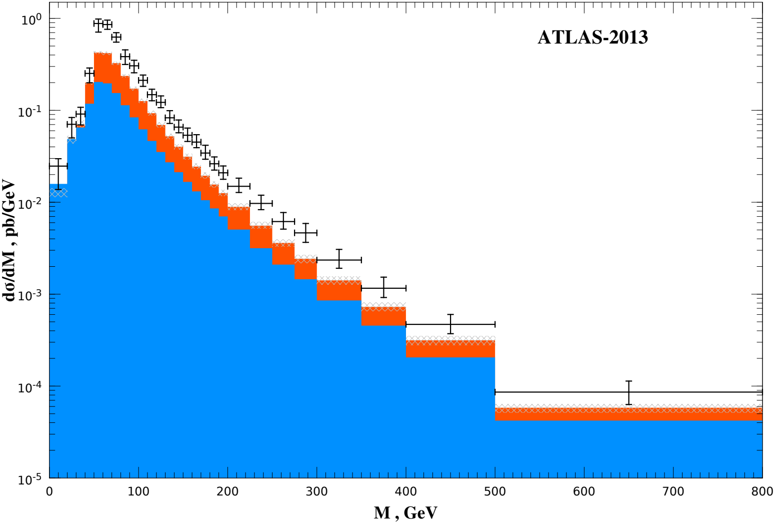

Conclusions.

- The good description of experimental data is achieved in the $p_T > M$-region, already in the LO of PRA.
- In this kinematical region, NLO QMRK corrections are shown to be supressed, demonstrationg the self-consistency of the approach.
- Our results demonstrate, why in many other processes, like single photon, jet or heavy quarkonia production, the LO PRA calculations describe data well.
- The $RR \to \gamma\gamma$ contribution is shown to be $30 - 40\%$ smaller than in the CPM case, constituting $O(10\%)$ of the cross-section.